Feedback Isolation by Piezoelectric Transformers: Comparison of Amplitude to Frequency Modulation

Simon Lineykin and Sam Ben-Yaakov*

Power Electronics Laboratory
Department of Electrical and Computer Engineering
Ben-Gurion University of the Negev
P. O. Box 653,Beer-Sheva 84105, ISRAEL, Phone: +972-8-646-1561,Fax: +972-8-647-2949
Email: sby@ee.bgu.ac.il, Website: www.ee.bgu.ac.il/~pel

Abstract - **Signal isolation is needed in power electronics systems that include separate primary and secondary 'grounds'. The feasibility of using a piezoelectric transformer (PT) as a galvanic barrier was investigated in this study theoretically and experimentally. The research included the issues of drive, demodulation, bandwidth, and common mode rejection. In particular, two types of excitation signals were compared: amplitude modulated and frequency modulated. The frequency response of the piezoelectric isolator was studied by small signal envelope simulation using ORCAD/PSPICE as well as experimentally. It is concluded that the FM approach offers a larger BW but the AM scheme seems to be easier to implement.**

I. INTRODUCTION

Signal isolation is needed in power electronics systems that include separate primary and secondary 'grounds' [1], [2]. Conventional solutions to the signal isolation problem include galvanic isolation by opto-couplers, capacitors, or transformers (Fig 1). In this study, we explored the feasibility of using a ceramic Piezoelectric Transformer (PT) [3] as the barrier element. That is, the possibility of replacing the isolation element by the PT [4]. Since the PT cannot transfer low frequency and DC signal, modulation techniques need to be applied. Namely, the error signal is first used to modulate a carrier and then recovered by demodulating the output signal past the isolation barrier. This is similar to the method used when an electromagnetic transformer is applied to realize the isolation barrier. The primary objective of this investigation was to compare the PT isolator performance in terms of the small signal bandwidth of the PT transfer function, when modulated by AM or FM signals (Fig. 2).

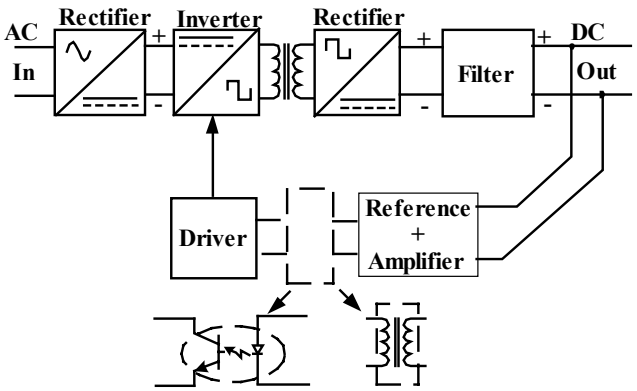

Fig. 1. Conventional feedback isolation in power converters.

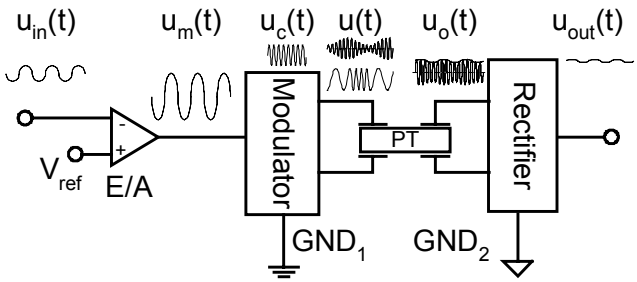

Fig. 2. Block-diagram of a PT-Isolator with FM or AM excitation.

II. THE PIEZOELECTRIC TRANSFORMER

The PT is a solid-state device that transforms the electrical energy at its input port to a secondary electrical energy at the output port using acoustic waves as a medium. The PT operates at frequencies that are close to its mechanical resonance so the PT is, in fact, a selective resonant system. The equivalent circuit of a Fig. 3 describes the PT for a given resonant mode [3], [5], [6]. It includes a resonant network (L_r, C_r, R_m) that emulates the effect of the mechanical vibration and dependent sources that express the gain. The model also comprises the physical dielectric capacitors (C_{in}, C_o), which are formed by the input and output electrodes. Also included in this model are stray capacitances C_{nm} (n,m=1,2) between input and output electrodes. These capacitances play an important role in deteriorating the Common Mode Rejection Ratio (CMRR) of the device. That is, the ratio between the differential and the common mode transfers. High common mode signal penetration will not only deteriorate the signal to noise ratio at the output but will also increase the EMI signal at the output section and will therefore require extra filtering to satisfy common standards.

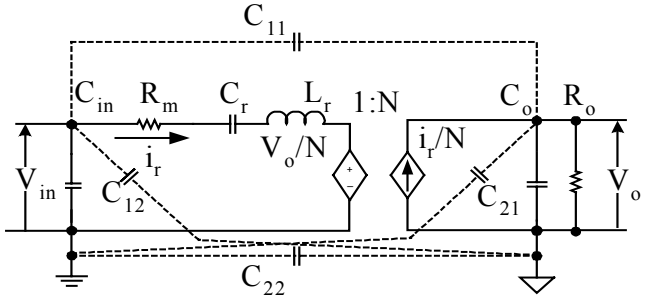

Fig. 3. Equivalent circuit of a piezoelectric transformer (PT) loaded by R_o. For experimental PT: C_{in}=200pF, C_o=220pF, L_r=16.58mH, C_r=12.97pF, R_m=910Ω, and N=1.2 (Q_m=49.3, f_r=342.9kHz, f_s=354.8kHz). C_{nm} are parasitic capacitive couplings between input and output electrodes.

* Corresponding author.

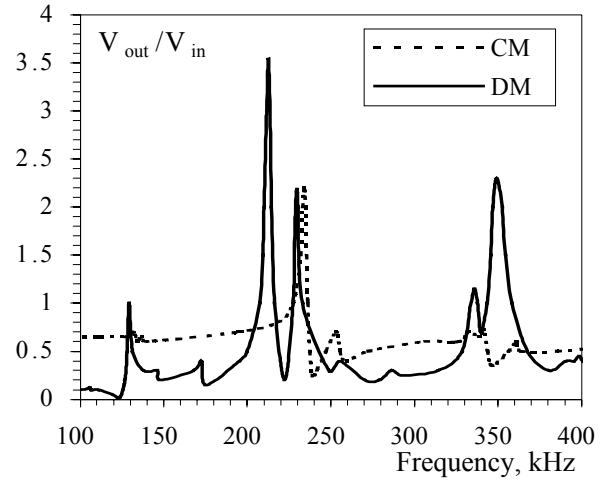

Fig. 4. Differential Mode (DM) and Common Mode (CM) transfer ratios of experimental PT.

In this study, we have used a small size PT (2x2x3mm) made of Lead Zirconate Titanate material EC65. The transfer functions of the experimental PT are shown in Fig. 4. The plots suggest that the peak at 350 kHz is a good choice since it is a conveniently high frequency and has the best CMRR. A closed look at the differential mode transfer function of the PT (Fig. 5) reveals that the peak around the chosen operating frequency (350kHz) is adjacent to another peaks in the vicinity. In the following, though, it is assumed that the PT can be represented to reasonable degree by a single resonant network.

III. Extracting the PT Parameters

The common method for studying the behavior of systems that include different energy types is to build an electrical equivalent circuit, which emulates the behavior of the complete system. The advantage of the equivalent circuit is that it can be studied by means of traditional techniques of electronic circuits analysis. Several methods have been proposed for extracting the equivalent circuit parameters of a PT [5], [6], [7]. The proposed method used in this study was motivated by the need to get the parameters of a PT of moderately low mechanical quality factor Q_m using minimum number of measurements and simple equipment.

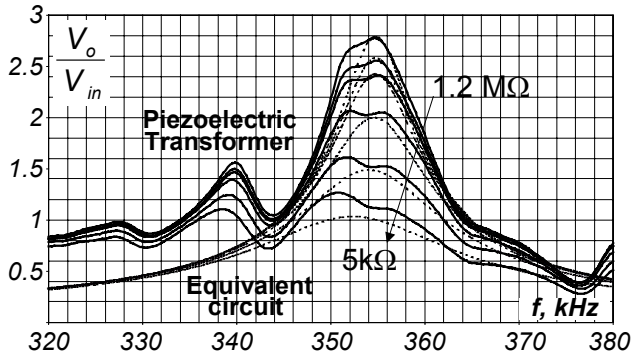

Fig. 5. Gain versus frequency of experimental PT (solid lines) and transfer function of equivalent circuit (dashed lines) of Fig. 3 for the loads: 1.2MΩ, 100kΩ, 56kΩ, 22kΩ, 10kΩ, and 5kΩ.

The method applies the measurement of the maximum of output to input voltage ratio for unloaded PT and when loaded with a known arbitrary load, and the frequencies of corresponding maxima.

The calculation of the equivalent circuit elements was based on the following assumptions:

1. There is only one significant resonant mode around the frequency of operation. The influence of other frequencies is negligible.
2. The input resistance of the measuring equipment is large enough so the loading effect can be neglected.
3. ESRs of input and output capacitors are small and may be neglected.
4. Output capacitance C_o of the secondary electrode pair is known.
5. There are four unknown elements in the equivalent circuit: C_r, L_r, R_m, and N (see Fig. 3).

For the equivalent circuit of Fig. 3, the output to input voltage ratio is expressed as (1)

$$A(R_o, f) = \frac{V_o}{V_{in}} = \sqrt{\frac{C_r^2 N R_o^2 \omega^2}{F}} \tag{1}$$

where:

$$F = \left(N^2 - C_r L_r N^2 \omega^2 - C_o C_r N^2 R_m R_o \omega^2\right)^2 + \left(C_r N^2 R_m \omega + C_r R_o \omega + C_o N^2 R_o \omega - C_o C_r L_r N^2 R_o \omega^3\right)^2 \tag{2}$$

$$\omega = 2\pi f \tag{3}$$

and f is frequency.

The frequency at which the transfer ratio reaches a maximum, f_{max}, can be derived by differentiating (1) with respect to f and solving for the roots of the resulting equation (4)

$$2C_r^2 N^6 R_o^2 - 4C_o^2 C_r^4 L_r^2 N^6 R_o^4 x^3 - \left(\begin{matrix} 2C_r^4 L_r^2 N^6 R_o^2 + 4C_o C_r^4 L_r N^4 R_o^4 + \\ 4C_o^2 C_r^3 L_r N^6 R_o^4 - 2C_o^2 C_r^4 N^6 R_m^2 R_o^4 \end{matrix}\right) x^2 = 0 \tag{4}$$

where

$$x = (2\pi f_{max})^2 \tag{5}$$

The simplified equivalent circuit of the open-circuited PT (Fig. 6) was derived from the previous expression by setting the resistance of the load resistor R_O to infinity. The transfer function was found to be:

$$A(\infty, f) = \left.\frac{V_o}{V_{in}}\right|_{R_o \to \infty} = \frac{NC_r}{\sqrt{C_r^2 C_o'^2 R_m^2 \omega^2 + \left(C_r + C_o'\left(1 - C_r L_r \omega^2\right)\right)^2}} \tag{6}$$

where

$$C_o' = C_o \cdot N^2 \tag{7}$$

Output voltage of Fig. 6 is:

$$V_o' = \frac{V_o}{N} \tag{8}$$

By differentiating expression (6) with respect to ω and equating the resulting expression to zero, the angular frequency of the maximum of the transfer function of open circuited PT, f_{pk} was obtained as:

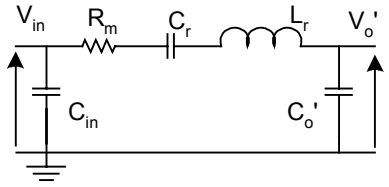

Fig. 6. Simplification of the equivalent circuit of the open-circuited PT.

$$\omega_{pk} = \sqrt{\frac{C_o' + C_r}{C_o' C_r L_r} - \frac{R_m^2}{2L_r^2}} = \sqrt{\frac{C_o' + C_r}{C_o' C_r L_r}\left(1 - \frac{1}{2Q^2}\right)} \approx \sqrt{\frac{C_o' + C_r}{C_o' C_r L_r}} \tag{9}$$

where

$$Q = \frac{1}{R_m}\sqrt{\frac{L_r}{C_r}}\sqrt{1 + \frac{C_r}{C_o'}} \tag{10}$$

and

$$f_{pk} = \omega_{pk}/2\pi \tag{11}$$

f_{pk} is the frequency of maximum input to output ratio of the unloaded PT. Q is a quality factor of the open-circuited PT, usually larger than five. Hence, the frequency of the peak of the transfer function of the open-circuited PT is very close to the series resonance frequency f_s ($\omega_s = 2\pi f_s$).

$$\omega_{pk} \approx \omega_s = \sqrt{\frac{C_o + C_r N^2}{L_r C_r C_o}} = \frac{1}{\omega_r}\sqrt{1 + \frac{C_r}{C_o'}} \tag{12}$$

where

$$\omega_r = 1/\sqrt{L_r C_r} \tag{13}$$

ω_r- the angular frequency of the mechanical resonant circuit ($\omega_r = 2\pi f_r$).

Consequently, the output to input voltage ratio at the frequency of maximum is $A(\infty, f_{pk})$

$$A(\infty, f_{pk}) = \frac{N}{R_m}\frac{2L_r\sqrt{C_r}}{\sqrt{C_o'\left(4L_r(C' + C_r) - C_r C_o' R_m^2\right)}} \approx \approx \frac{N}{R_m}\sqrt{\frac{C_r L_r}{C_o'(C_o' + C_r)}} \tag{14}$$

Solving together equations (6 - 14), one obtains:

$$R_m = \frac{Q\left(f_{pk}^2 - f_r^2\right)}{2\pi C_o A(\infty, f_{pk})^2 f_{pk}^3} \tag{15}$$

$$C_r = \frac{A(\infty, f_{pk})^2 C_o f_{pk}^4}{\left(f_{pk}^2 - f_r^2\right) f_r^2 Q^2} \tag{16}$$

$$N = \frac{A(\infty, f_{pk}) f_{pk}^2}{\left(f_{pk}^2 - f_r^2\right) Q} \tag{17}$$

$$L_r = \frac{\left(f_{pk}^2 - f_r^2\right) Q^2}{4\pi^2 f_{pk}^4 C_o A(\infty, f_{pk})^2} \tag{18}$$

The above solutions apply the two measured values of the open-circuited PT: $A(\infty, f_{pk})$ and f_{pk}, and assume that Q and f_r are known.

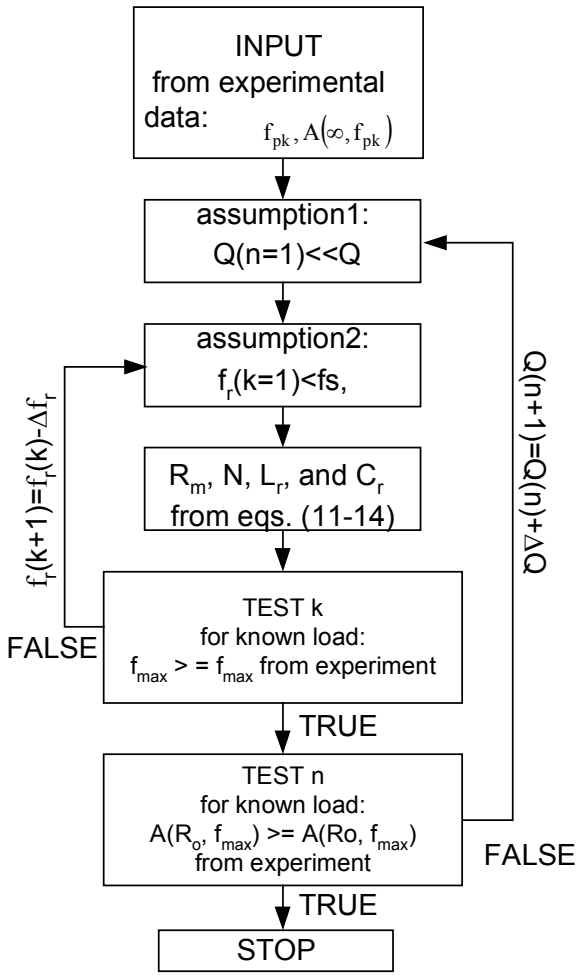

Fig. 7. Block diagram of the algorithm for estimating the parameters of a PT equivalent circuit.

The exact numerical values of parameters can be evaluated by an iteration procedure. The iteration process starts after assuming some initial values for Q and f_r and plugging them in (15-18) which are evaluated. The results are then used to estimate f_{max} and $A(R_o, f_{max})$ and these are compared to the measured values. In a case of mismatch, Q and f_r are incremented and the calculation is repeated.

The block-diagram of the iteration algorithm is shown in Fig. 7. Once the procedure converges to the solutions, one needs to check the validity of the apriori assumptions: that Q is larger than five and that the input resistance of the measuring equipment R_{in} is equal or larger than the output impedance of the PT:

$$R_{in} \geq \frac{50 + \sqrt{2500 - N^4 4\pi^2 f_r^2 C_o^2 R_m^2}}{N^4 4\pi^2 f_r^2 C_o^2 R_m} \tag{19}$$

Applying the above procedure on the experimental PT, the following parameters were extracted: L_r=16.58mH, C_r=12.97pF, R_m=910Ω, and N=1.2 (Q_m=49.3, f_r=342.9kHz, f_s=354.8kHz). Input and output capacitances were measured as: C_{in}=200pF, C_o=220pF. The transfer function of the re-modeled equivalent circuit is shown in Fig. 5 by dashed lines for different loads and is found to be in good agreement with the experimental data (solid lines).

IV. MODULATION SCHEMES

In this study, we explored two modulation alternatives: amplitude modulation (AM) and frequency modulation (FM) (see Fig. 2). In the AM case, a constant frequency carrier is used and by varying the amplitude of the carrier, the error signal is transmitted. In the FM case, the error signal is coded into a frequency deviation that is translated at the output of the PT into an amplitude change.

A. Frequency Modulation

For single-tone harmonic modulating signal m(t)

$$m(t) = M\cos\omega_m t \tag{20}$$

where ω_m is angular frequency of the modulating signal $\omega_m=2\pi f_m$, and M is its amplitude, one can express the modulated carrier wave v(t):

$$v(t) = A_c\cos(\omega_c t + K\int_0^t m(t)dt) \tag{21}$$

where ω_c and A_c are angular frequency and amplitude of the carrier signal and K is the modulation coefficient. Or, after integration:

$$v(t) = A_c\cos(\omega_c t + \left(\frac{KM}{\omega_m}\right)\sin\omega_m t) \tag{22}$$

$$\frac{KM}{\omega_m} = \beta \tag{23}$$

The spectrum of a frequency-modulated signal includes the fundamental term at the frequency of the carrier signal and an infinite set of side-frequencies located symmetrically on either side of the carrier at frequency separations of f_m, $2f_m$, $3f_m$, etc. For a small modulating signal of small amplitude ($\beta<<1$) (narrow band frequency modulation - NBFM), only two sidebands (f_c+f_m) and (f_c-f_m) have significant values. Thus, the required bandwidth (BW) to transfer a modulating signal of frequency f_m is:

$$BW = 2f_m \tag{24}$$

B. Amplitude Modulation

For the single-tone amplitude modulation m(t) of (20)

$$v(t) = (1 + k_a m(t))A_c\cos(\omega_c t) \tag{25}$$

where k_a is the modulation index. Or:

$$v(t) = A_c\cos(\omega_c t) + k_a A_c M\cos(\omega_m t)\cos(\omega_c t) \tag{26}$$

And after some trigonometric transformations:

$$v(t) = A_c\cos(\omega_c t) + \frac{k_a A_c M}{2}\cos((\omega_c - \omega_m)t) + \frac{k_a A_c M}{2}\cos((\omega_c + \omega_m)t) \tag{27}$$

Hence, the spectrum of an AM signal will include of a carrier (f_c) plus two side bands located at f_c+f_m and f_c-f_m where f_m is the modulating frequency. Thus, like in the case of narrow band FM, one can express the required bandwidth for passing m(t):

$$BW = 2f_m \tag{28}$$

It can thus be concluded that for small signal analysis, both the AM and FM scheme require the same bandwidth for a given modulating signal f_m. However, since the PT is a resonant element, its gain is frequency dependent. As a result, the carrier and side bands of the modulated signal will be attenuated differently and this may affect the practical BW that can be obtained via the PT. It could further be expected that the location of the carrier frequency in relation to the PT's maximum gain frequency, will also have an impact on the BW. These questions were studied by envelope simulation and then verified experimentally.

V. SMALL SIGNAL ENVELOP SIMULATION

The question of small signal bandwidth of a PT when passing a modulated signal can conveniently be studied by small signal envelope simulation [8]. In this technique, the original signal is broken into two coupled parts, a real and imaginary network.

As demonstrated in [8], the SPICE compatible small-signal envelope simulation circuit can be developed by means of the following stages:

1. Duplicating the circuit to create the real and the imaginary parts.
2. In the two sections: replacing reactive elements (L, C) into the real and imaginary sections of the circuit, as shown in Fig. 8.
3. Placing two excitation sources for real and imaginary parts in according to the type of modulation as shown in Fig. 9.
4. Adding a behavioral element for calculating the square root of the sum of squares of real and imaginary components of the output signals.

Using this technique, the equivalent circuit of Fig. 3 was transformed into the SPICE compatible circuit of Fig. 10. This circuit is valid for AM as well as FM excitation. The only difference is the source element for FM (Fig. 9(a)) and for AM (Fig. 9(b)). This circuit was than used to explore by simulation the transfer of a modulated signal via the PT.

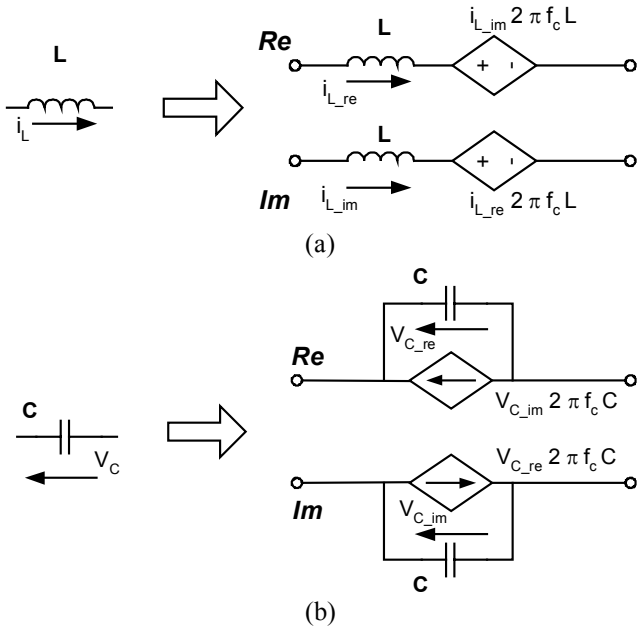

Fig. 8. Replacement of reactive elements by equivalent circuits for envelope simulation: (a)-Replacing an inductor by an inductor and dependent voltage source; (b)-Replacing a capacitor by a capacitor and dependent current source.

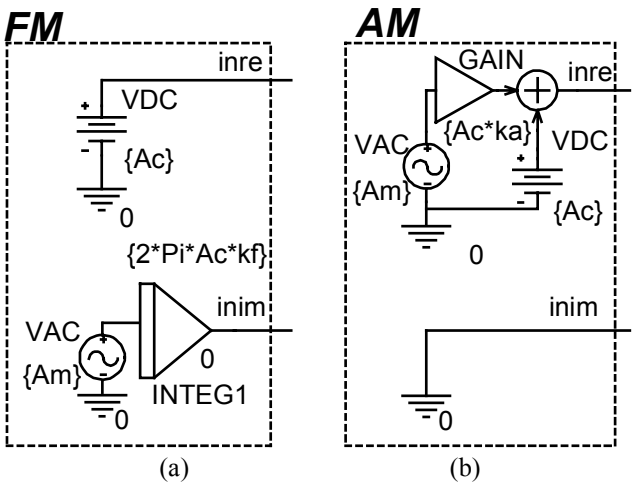

Fig. 9. Real and imaginary components of the source for small-signal envelope simulation, those represent excitation by FM (a) and AM (b). Ac - amplitude of the carrier wave, Am - amplitude of the modulating signal, kf – coefficient of frequency modulation, ka – coefficient of amplitude modulation, Pi is π.

VI. Simulation And Experimental Results

The small signal transfer function of the PT under study was measured by the experimental setup of Fig. 11. The PT was driven by a modulated signal, the output was buffered (to control loading), rectified by a voltage doubler and the rectified signal was buffered again.

Typical results of the experimental measurements (fine line) and simulations (heavy lines) are shown in Fig. 12 and Fig. 13 The good agreement between the experimental and simulation results support the conjecture that small signal envelope simulation is a viable tool to explore the BW of a PT under various modulating conditions.

The experimental and simulation results demonstrate that the tested PT has a BW of about 5-7kHz both in AM and FM excitation. However, the results show that the location of the carrier frequency in relation to the resonant frequency affects the transfer function of the PT. In particular, whereas AM works well if the carrier and resonant frequencies coincide, better results are obtained for FM when the carrier is off the resonant frequency. To test this point we have run additional experiments and simulations. The results (Fig. 14) show that around the peak, the BW is the smallest and that larger BW is obtained off peak. This can be explained by the fact that the high frequency side bands are highly attenuated when the carrier frequency is at the peak of the transfer function. Results of small signal envelop simulation for both excitation types coincide. However, in practice, it was not possible to measure the transfer function of FM excitation when the carrier frequency was too close to the resonant frequency while the AM results were inconsistent when the carrier frequency was far from the resonance frequency peak. Fig. 14 shows the combined results of the simulation and experiments for the relevant excitation carrier frequencies.

Experiments were also run to determine the Common Mode Rejection (CMRR), that is, the ratio of differential mode gain (DM) to the common mode gain CM, of the PT over the chosen frequency of operation. The results (Fig. 15) suggest that the CMRR for this PT is in the range of 10db.

VII. Discussion and Conclusions

The main advantages of the PT in the proposed application are the small size and the very high isolation breakdown voltage that can be achieved. This is due to the good isolation of the ceramic material. The main disadvantage is the common mode stray capacitance between primary and secondary sides of the PT. The measured CMRR of about 10db (Fig. 15) may be too high in the noisy environment of a

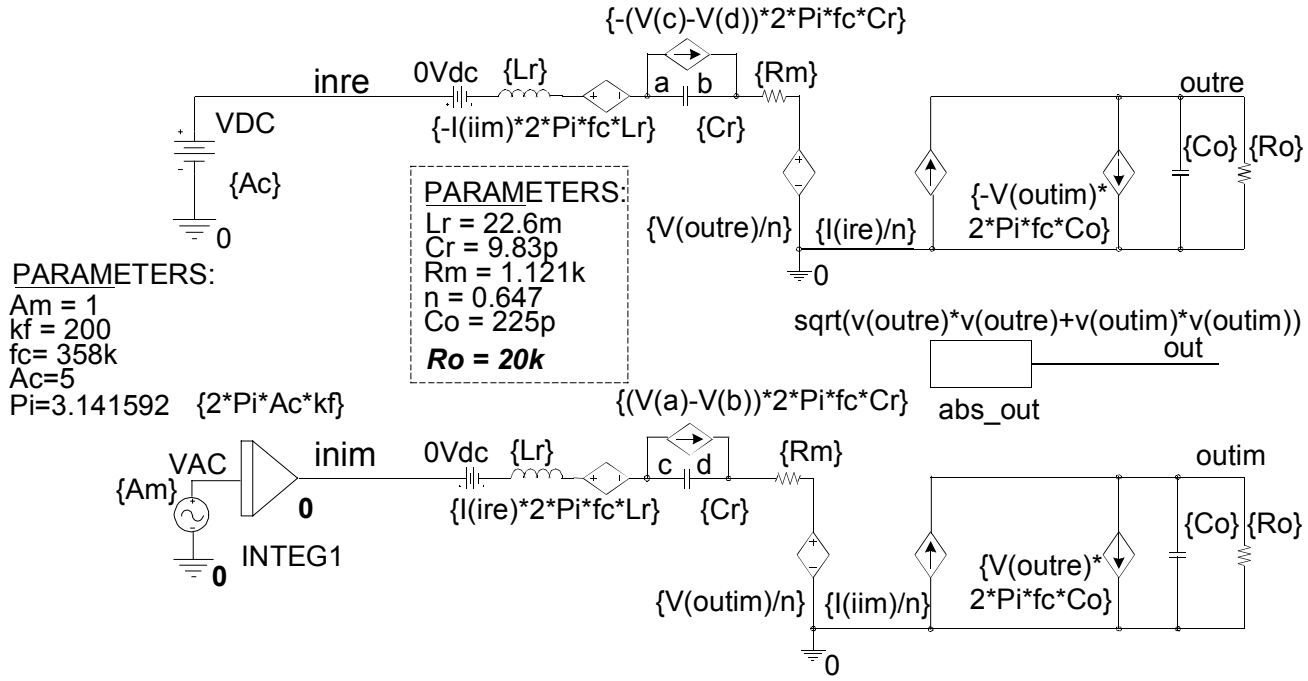

Fig. 10 ORCAD/PSPICE (Version 9.2) schematics for AC-Envelope simulation of experimental PT excited by an FM signal.

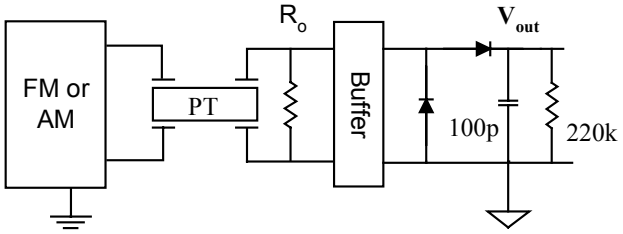

Fig 11. The experimental setup.

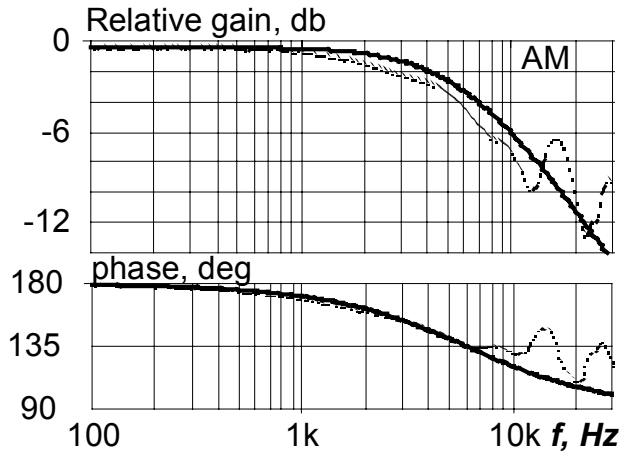

Fig. 12. Small signal transfer function of the experimental PT in AM scheme. Solid line: small signal envelop simulation. Dashed line: experimental. Carrier frequency: 353kHz

switch mode converter, if there is a significant common mode signal across the isolator. The possible interference of the common mode signal can be minimized by proper design, for example by connecting the primary of the isolator to a quite 'ground' with respect to the ground of the output. The common mode rejection could be further improved by ensuring that the harmonics of the switching frequency of the converter do not coincide with the common mode peaks of the PT.

The present study suggests that both AM and FM can be used to pass feedback signals via an isolation PT. It was found that the small signal bandwidth of both excitation cases is practically the same. However, the experiments that were carried out with practical finite signals, as opposed to infinitesimally small modulating signal assumed in small signal envelop simulation, reveal a difference between the AM and FM schemes. It was found that in the AM option, best results were obtained when the carrier frequency was close to the resonant frequency (Fig. 12). When the carrier was off the resonance frequency of the PT, the demodulated signal was highly distorted. The inverse was found in the case of FM. In this case, best results were obtained when the carrier frequency was off the peak of the resonance (Fig. 13). Since a higher BW is obtained off resonance, the FM approach is better in this respect. However, the AM scheme might have a practical advantage since it is possibly simpler to realize by self-oscillating circuit that locks to a frequency that is close to the resonant frequency. Another possible frequency tracking technique is described in [9]. In the FM case, one would need to stay off resonance, which

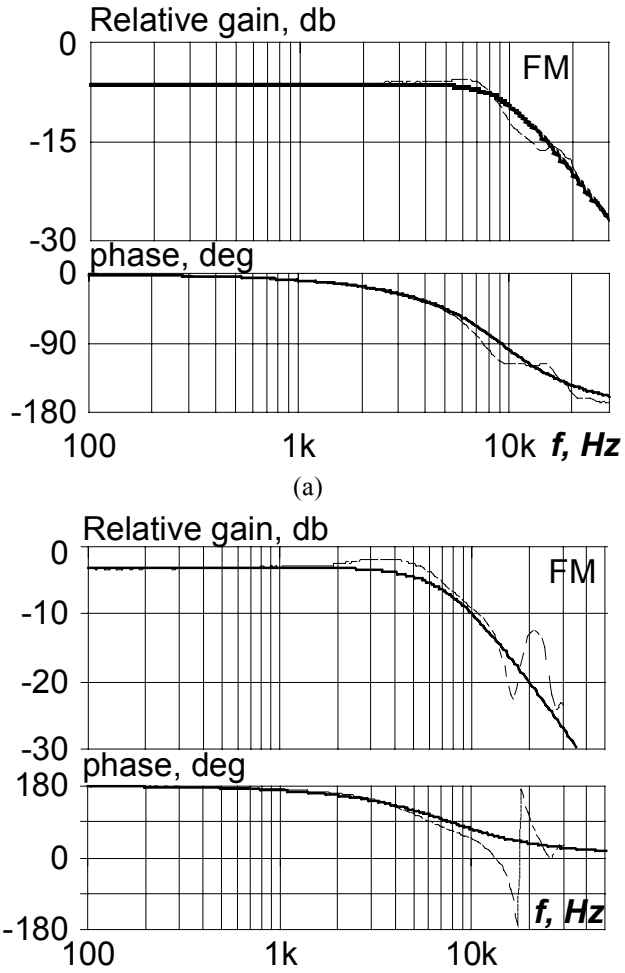

Fig. 13. Small signal transfer function of the experimental PT in FM scheme. Solid line: small signal envelop simulation. Dashed line: experimental. Carrier frequency: (a) – f_c = 346.1kHz, (b) - f_c = 357.7 kHz.

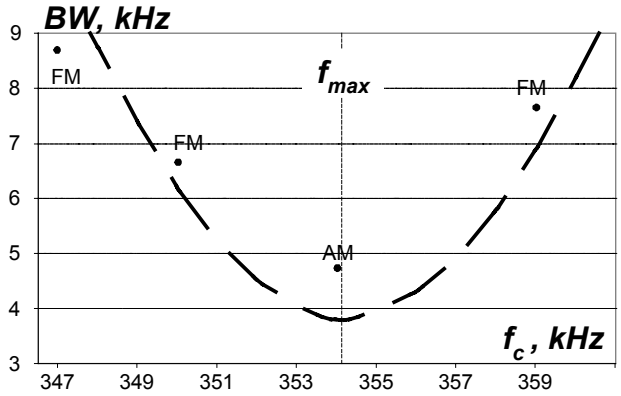

Fig. 14. Bandwidth (BW) of the PT transfer function for AM and FM modulated signal versus frequency of the carrier signal. Simulation: line. Experimental measurements: dots.

might pose a problem considering the spread and temperature dependence of the PT parameters. It can thus be concluded that the FM approach offers a larger BW but the AM seems to be easier to implement.

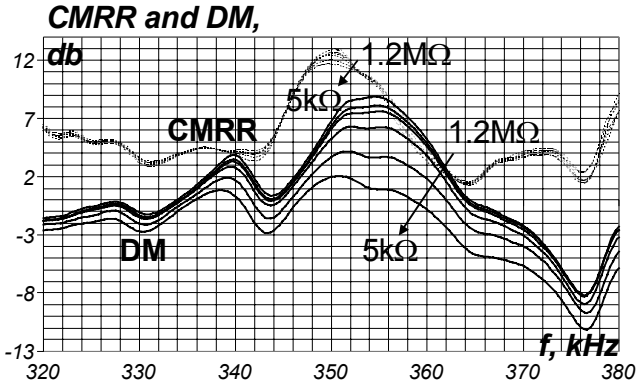

Fig. 15. Differential-mode (DM) signal and CMRR of the experimental PT for different loads (5kΩ to 1.2MΩ) in the frequency range close to resonance.

ACKNOWLEDGMENT

This research was supported by THE ISRAEL SCIENCE FOUNDATION (grant No. 113/02) and by the Paul Ivanier Center for Robotics and Production management.

REFERENCES

[1] M. Zirngast, "Capacitive isolation expands analogue design options-Part 1," *Electronic-Engineering- (London)*, vol. 61, no. 748, pp. 37 - 40, Apr 1989.

[2] M. Zirngast, "Capacitive isolation expands analogue design options-Part 2," *Electronic-Engineering- (London)*, vol. 61, no. 749, pp. 33 - 45, May 1989.

[3] G. Ivensky, I. Zafrany, and S. Ben-Yaakov, "Generic operational characteristics of piezoelectric transformers," *IEEE Transactions on Power Electronics,* vol. 17, no. 6, pp. 1049-1057, November 2002.

[4] S. Lineykin and S. Ben-Yaakov, "Feedback isolation by piezoelectric transformers: a feasibility study," *Power Conversion and Intelligent Motion, PCIM-2000*, pp. 175-181, June 2000.

[5] R. Holland and E. Eernisse, *Design of resonant piezoelectric devices*, Cambridge: The M.I.T. Press, 1966.

[6] An American National Standard, *IEEE standard on piezoelectricity*, ANSI: IEEE std. 176, 1978

[7] J. Merhaut, *Theory of electroacoustics*, New York: McGraw-Hill Book Company, 1981.

[8] S. Lineykin and S. Ben-Yaakov, "A Unified SPICE compatible model for large and small signal envelope simulation of linear circuits excited by modulated signals," *PESC-2003*, pp. 1206-1209, June 2003.

[9] S. Ben-Yaakov and S. Lineykin, "Frequency tracking to maximum power of piezoelectric transformer HV converters under load variations," *PESC-2002*, pp. 657-662, June 2002.